The effect of alkaline pretreatment on surfactant-modified clinoptilolite for diclofenac adsorption: isotherm, kinetic, and thermodynamic studies

Fateme Poorsharbaf Ghavi, Fereshteh Raouf and Ahmad Dadvand Koohi

ABSTRACT

The elimination of diclofenac traces from aqueous environments is important. In this research, the effect of alkaline (NaOH) pretreatment on clinoptilolite before its modification with a surfactant (HDTMA) for diclofenac adsorption under the speculation of the sole presence of diclofenac in the aqueous solution is investigated. The results are compared through isotherm, kinetic, and thermodynamic studies and supplemented by Fourier transform infrared spectroscopy (FTIR), scanning electron microscopy (SEM), Brunauer–Emmett–Teller (BET), and the zeta potential analyses. The contact time was investigated in a 0–180-min range. The pH effect was studied in a range of 5–10 because of diclofenac dissociation below pH = 5. The effect of the temperature on diclofenac adsorption was also considered by establishing the experiments at 25, 35, and 45 °C. For HDTMA-modified clinoptilolite, Temkin, and for NaOH-HDTMA-modified clinoptilolite, Dubinin–Radushkevich, and Freundlich isotherm models and in both cases, the pseudo-second-order kinetic model fitted the experimental data best. All the enthalpy and the entropy changes were negative, suggesting exothermic adsorption with a decrease in the degree of freedom of diclofenac anions after the adsorption. Furthermore, diclofenac physisorption was confirmed through isotherm and kinetic studies.

Key words | adsorption, alkaline pretreatment, clinoptilolite, diclofenac, HDTMA

Fateme Poorsharbaf Ghavi
Fereshteh Raouf (corresponding author)
Ahmad Dadvand Koohi
Department of Chemical Engineering,
University of Guilan,
Rasht,
Iran
E-mail: *f.raouf@guilan.ac.ir*

HIGHLIGHTS

- Incapability of clinoptilolite for diclofenac adsorption.
- Increase in total pore volume of clinoptilolite after NaOH pretreatment; confirmed by BET analysis.
- Effective clinoptilolite modification with HDTMA.
- Change in surface charge through HDTMA loading; confirmed by zeta potential analysis.
- Slight enhancement in maximum diclofenac adsorption capacity for NaOH-HDTMA-Clino compared with HDTMA-Clino.

INTRODUCTION

As the human population increased during recent years, the need for drinking water supplies grew. Some pharmaceuticals escape the wastewater treatments and pollute the rivers; they can remain in water resources and threaten the ecosystem (Akhtar *et al.* 2016). Diclofenac (DCF) is an acidic pharmaceutical which belongs to the non-steroidal pharmaceutical group with an analgesic effect. It is prescribed for arthritis, rheumatism, and after-surgery inflammations (Sotelo *et al.* 2014). DCF is one of the most common pollutants in aqueous environments. It can be

degraded in surface waters by sunlight, but the formed products are more dangerous to other living organisms (Huguet *et al.* 2013).

Continuous uptake of DCF into the human body, even in low concentrations, causes body function failure (de Luna *et al.* 2017). The accumulation of DCF residues in human organs causes serious health problems such as kidney, liver, and tissue damages. The limit of detection of DCF is reported to be between 1 and 10 ng/L (Poorsharbaf Ghavi *et al.* 2020). Removal methods such as adsorption, oxidation, ozonation, and Fenton processes have been applied to eliminate pharmaceutical traces from the aqueous environments. Adsorption, however, is of more interest because of its simplicity and effectiveness (Hu & Cheng 2015). Zeolites are commonly used adsorbents because of their low cost and adsorptive characteristics. Zeolites have a net negative charge, so they have no or low affinity toward anions (Warchoł *et al.* 2006). Surfactants are molecules with long chains and have both hydrophobic and hydrophilic parts (Urum & Pekdemir 2004). In an aqueous solution, the surfactant forms aggregations at a specific concentration. This is the critical micelle concentration (CMC). The surface ion exchange capacity of the zeolite increases as a result of zeolite modification by surfactants; thus, the surfactant-modified zeolite shows a better function in the adsorption of anions and organic compounds (Misaelides 2011).

Hexadecyltrimethylammonium bromide (HDTMA-Br) is a cationic surfactant (Jiménez-Castañeda & Medina 2017). The adsorption of HDTMA on clinoptilolite consists of two major steps: (1) the HDTMA micelles are adsorbed directly on the clinoptilolite surface and (2) the adsorbed HDTMA molecules rearrange to form monolayers or bilayers. If the initial concentration of HDTMA is less than its CMC, monolayers appear, and if it is more than the CMC, admicelles form on the adsorbent surface. These admicelles then rearrange and bilayers appear. In bilayers, the positive head of HDTMA tends to be toward the solution. This helps the modified adsorbent to adsorb anions (Ambrozova *et al.* 2017). Alkaline treatment with NaOH has proven to increase the cation exchange capacity of zeolite and if it is followed by a surfactant modification, the adsorbent effectively adsorbs organic compounds (Tran *et al.* 2018). Alkaline pretreatment can be used for other

purposes such as the bioconversion of lignocellulosic biomass. This pretreatment is advantageous, as it can simply be carried out under ambient temperature, it is cheap, and the procedure is easy to exploit (Kim *et al.* 2016). The modification of clinoptilolite with NaOH increases its sodium content, and the presence of the sodium cations can improve the cation exchange capacity of clinoptilolite (Ates & Akgül 2016).

The literature review showed that HDTMA-modified clinoptilolite (HDTMA-Clino) was an effective adsorbent for DCF. On the other hand, alkaline pretreatment of a zeolite improved its characteristics as an adsorbent through the enhanced surface area. The combination of these two modification methods and the comparison between them for DCF adsorption were missing from previous studies, so this study focuses on DCF adsorption with HDTMA-Clino and NaOH-HDTMA-modified clinoptilolite (NaOH-HDTMA-Clino). The feasibility of HDTMA-Clino and NaOH-HDTMA-Clino for DCF adsorption in the aqueous solution is assessed under different experimental conditions, by varying the contact time, the pH of the solution, the adsorbent amount, the initial DCF concentration, and the temperature. The experimental data are studied alongside with the results from different analyses of the adsorbents to reach reliable conclusions.

MATERIALS AND METHODS

DCF sodium with $C_{14}H_{10}Cl_2NNaO_2$ molecular formula and 318.129 g/mol M_w was prepared (from Behdashtkar Company in Guilan, Iran; coded as B.DF.87.130) and used as an analytical grade. Clinoptilolite was prepared, modified, and used as the adsorbent (purchased from Afrazand Tooska Company in Semnan, Iran). The clinoptilolite had an average particle size of 600 μm and a SiO_2/Al_2O_3 ratio equal to 6.73. HDTMA-Br was used for clinoptilolite modification (purchased from Merck in Germany; CAS-No: 57-09-0). Powdered NaOH ($M_w = 40$ g/mol) was used to prepare NaOH solutions for the adsorbent alkaline pretreatment. Diluted NaOH and HCl solutions were used to adjust pH. A WPA UV–visible spectrophotometer (Biowave II) was used to detect the concentration of the

solutions. A quartz cuvette was used in spectrophotometry (purchased from Azin Laboratory in Tehran, Iran).

In order to modify the clinoptilolite, 5 g of clinoptilolite was added to a series of 100 mL HDTMA solutions with concentrations equal to 1, 2.5, 5, 15, and 25 CMC (CMC = 0.93 mmol/L (Cifuentes *et al.* 1997)). The solutions were shaken in an incubator shaker for 24 h at 200 rpm and 25 °C. The modified adsorbent was washed several times. The DCF removal percent with HDTMA-Clino with different amounts of the loaded HDTMA was compared, and the appropriate amount of HDTMA for modification was chosen.

To investigate the effect of alkaline pretreatment on the adsorbent characteristics, two modification conditions were adjusted. In the first set of conditions, 4 g of clinoptilolite was added to a 1.5 mol/L NaOH solution and mixed in an incubator shaker at 200 rpm and 25 °C for 24 h. In the second set of conditions, 4 g of clinoptilolite was added to a 1.5 mol/L NaOH solution and mixed at 260 rpm and 55 °C for 90 min. After the alkaline pretreatment, the adsorbent was washed with distilled water until the solution pH was near 7. Then, the NaOH-pretreated clinoptilolite was modified by HDTMA. DCF adsorption with NaOH-HDTMA-Clino prepared under these two sets of conditions was compared, and the proper set was selected.

The effect of the contact time, the pH of the solution, the adsorbent amount, and the temperature on DCF adsorption was investigated. The removal percent and the adsorption capacity of HDTMA-Clino and NaOH-HDTMA-Clino for DCF adsorption were investigated at 20, 50, and 80 mg/L DCF solutions in a contact time range of 0–180 min. The effect of the solution pH was studied in a pH range of 5–10 for 50 mg/L DCF solutions and 0.5 g adsorbent in 100 mL volume. The effect of the adsorbent amount was studied with 0.5, 1, 1.5, and 2 g of HDTMA-Clino and NaOH-HDTMA-Clino for 50 mg/L DCF solutions. All the pH and the adsorbent amount investigation experiments were done at 25 °C and 200 rpm, at the equilibrium time. Also, the effect of DCF initial concentration and the temperature was investigated at three different temperatures: 25, 35, and 45 °C. The obtained experimental data were adjusted to Langmuir, Freundlich, Temkin, and Dubinin–Radushkevich (D–R) isotherm models to find the isotherm that explained the adsorption best. During all the isotherm

study experiments, the parameters were set in their optimum values, while the initial concentration and the temperature were the variables. To find the kinetic model that elucidated the DCF adsorption well, pseudo-first-order, pseudo-second-order, and intraparticle diffusion models were fitted to the experimental data and their deviations from the experimental data were calculated.

The Fourier transform infrared spectroscopy (FTIR) analysis was done using a Nicolet 560 FTIR spectrometer. A minimum amount of 50 mg of each powdered sample of clinoptilolite, HDTMA-Clino, and NaOH-HDTMA-Clino were prepared, and the FTIR spectra of these samples were obtained from 400 to 4,000 cm^{-1} to confirm the functional groups of the loaded surfactant. The scanning electron microscopy (SEM) images were taken by a Philips XL30 (WDX: WDX-3pc, Microspec) SEM device. The Brunauer–Emmett–Teller (BET) surface area, the total pore volume, and the average pore volume along with the related N$_2$ adsorption–desorption diagrams were obtained using a Belsorp mini II BET device for Microtrac Bel Corp. The zeta potential was determined by dispersing clinoptilolite, HDTMA-Clino, and NaOH-HDTMA-Clino in distilled water and using a ZetaCheck device for MicroTrac Company.

The removal percent was calculated with Equation (1) and the adsorption capacity was calculated with Equation (2):

$$\%R = \frac{(C_0 - C_e)}{C_0} \times 100 \tag{1}$$

$$q_e = \frac{(C_0 - C_e)}{m} \times V \tag{2}$$

In Equations (1) and (2), C_0 represents the initial concentration of the adsorbate and C_e represents the equilibrium concentration in terms of mg/L. Parameter m is the adsorbent amount in g, and V is the solution volume in L. %R shows the removal percent, and q_e is the equilibrium adsorption capacity of the adsorbent in mg/g.

Finding an isotherm that can explain the majority of the experimental data is important because it gives better insights to perceive the interactions between the adsorbate and the adsorbent. In the Langmuir isotherm model, the

adsorption is considered to be due to the physical and electrostatic forces. The adsorption takes place on monolayers on a homogenous adsorbent with identical adsorption sites (Wei *et al.* 2014). The Freundlich isotherm model, unlike Langmuir's, is valid for infinite adsorption which can take place on a heterogeneous adsorbent and does not determine the maximum adsorption capacity. This model is especially useful for the adsorption of organic pollutants (Fallou *et al.* 2016). The Temkin isotherm model is based on the assumption that the heat of the adsorption linearly decreases as the adsorption layers increase. This model also describes adsorption on a heterogeneous surface (Boparai *et al.* 2011). The D–R isotherm model is valid for adsorption on both the homogeneous and the heterogeneous surfaces. This model can predict the maximum adsorption capacity and the adsorption mechanism (El-Kamash 2008). The linear forms of the studied isotherm models and the related parameters are represented in Equations (3)–(10).

Langmuir isotherm can be represented by the following equation:

$$\frac{C_e}{q_e} = \frac{C_e}{q_m} + \frac{1}{K_L q_m} \tag{3}$$

In Equation (3), q_e is the equilibrium adsorption capacity and q_m is the maximum adsorption capacity; both in terms of mg/g. C_e is the equilibrium concentration of the adsorbate (mg/L), and K_L is the Langmuir adsorption constant (L/mg). Parameter R_L is the Langmuir dimensionless factor which indicates the adsorption characteristics. If $0 < R_L < 1$, it can be concluded that the adsorption was effective. Equation (4) shows how the R_L parameter can be calculated (Wei *et al.* 2014). In Equation (4), C_0 is the initial concentration in mg/L and K_L is the Langmuir adsorption constant (L/mg).

$$R_L = \frac{1}{1 + K_L C_0} \tag{4}$$

Equation (5) is for the Freundlich isotherm model:

$$\ln(q_e) = \frac{1}{n}\ln(C_e) + \ln(K_F) \tag{5}$$

In Equation (5), K_F is the Freundlich constant, which indicates the adsorption capacity (mg/g). $1/n$ shows the adsorption intensity and n is the deviation of the data from linear adsorption. If $n < 1$, the adsorption is chemisorption, and if $n > 1$, the process is physisorption. If $n = 1$, the adsorption is linear (Khambhaty *et al.* 2009).

Temkin isotherm is given by the following equations:

$$q_e = \beta \ln K_{T_e} + \beta \ln C_e \tag{6}$$

$$\beta = \frac{RT}{b} \tag{7}$$

In Equation (6), K_T is the equilibrium binding constant (L/g) and β is related to the heat of the adsorption. Equation (7) shows the calculation of β. In this equation, b is the adsorption energy in terms of J/mol, R is the universal gas constant and T is the absolute temperature in K (Boparai *et al.* 2011).

D–R isotherm is described by the following equations:

$$\ln(q_e) = \ln(q_D) - K\varepsilon^2 \tag{8}$$

$$\varepsilon = RT\ln\left(1 + \frac{1}{C_e}\right) \tag{9}$$

$$E = (2K)^{-1/2} \tag{10}$$

In Equation (8), q_D is the theoretical saturation capacity (mg/g), K is the D–R isotherm constant (mol²/J²) related to the mean adsorption energy, and ε is the Polanyi potential (J/mol). Equation (9) shows the relation for ε. In Equation (9), R is the universal gas constant, T is the absolute temperature, and C_e is the equilibrium concentration. To understand whether the adsorption is physical or chemical, the mean energy, E (J/mol), is calculated from Equation (10). If the E value is less than 8 kJ/mol, the adsorption is physisorption and if E is between 8 and 16 kJ/mol, chemisorption had occurred (El-Kamash 2008).

Studying the adsorption kinetics provides information about the rate of the adsorption and predicts the adsorption–desorption rate of the adsorbate in a solid–liquid system. The kinetic models which are commonly used to describe adsorption are pseudo-first-order, pseudo-second-order, and intraparticle diffusion. In the pseudo-first-order

kinetic model, the main resistance is related to the attachment of the adsorbate to the adsorption sites. Also, it is assumed that the rate of the adsorption sites being occupied is proportionate to the unoccupied sites. The pseudo-first-order kinetic model is given by the following equation:

$$\ln(q_e - q_t) = \ln q_e - k_1 t \tag{11}$$

In Equation (11), q_e is the equilibrium adsorption capacity and q_t is the adsorption capacity at t; and both are in terms of mg/g. K_1 is the reaction velocity constant (min^{-1}).

In the pseudo-second-order kinetic model, like the pseudo-first-order model, the main resistance to the adsorption is present in the attachment of the adsorbate to the adsorption sites. It is assumed that the rate of the adsorption sites being occupied is proportionate to the square of the unoccupied sites. The pseudo-second-order kinetic model can be expressed by the following equation:

$$\frac{t}{q} = \frac{t}{q_e} + \frac{1}{k_2 q_e^2} \tag{12}$$

In Equation (12), q_e is the equilibrium adsorption capacity and q is the adsorption capacity at t; both in units of mg/g. Parameter K_2 is the rate constant of the pseudo-second-order model in terms of g/(mg min) (Boparai *et al.* 2011).

It is indicated in the intraparticle diffusion model that the adsorption is proportionate to $t^{0.5}$. Equation (13) shows the relations between the parameters in the intraparticle diffusion model:

$$q_t = k_{id} t^{1/2} + c \tag{13}$$

In Equation (13), q_t is the adsorption capacity at t in terms of mg/g, K_{id} is the intraparticle diffusion rate constant in mg/(g min$^{0.5}$), and c is the equation constant which provides information about the boundary layer. The greater the parameter c is, the more the boundary layer affects the adsorption (Boparai *et al.* 2011).

In order to better understand different aspects of the adsorption, regarding its spontaneity, being endothermic or exothermic, and how the target ions rearrange toward smaller or greater degrees of freedom, it is important to study the thermodynamic of the process. Thermodynamic parameters such as the standard Gibbs free energy change ($\Delta G°$), the standard enthalpy change ($\Delta H°$), and the standard entropy change ($\Delta S°$) can be calculated according to the changes in the thermodynamic equilibrium constant (K_C), which itself is obtained via plotting $\ln(q_e/C_e)$ versus q_e and the extrapolation of q_e to zero. The changes in standard Gibbs free energy is calculated through the following equation, where T is the absolute temperature and R is the universal gas constant.

$$\Delta G° = -RT\ln K_C \tag{14}$$

$\Delta G°$ shows the spontaneity of the adsorption and the more negative it is; it means the process was more spontaneous. In order to gain the results of $\Delta H°$ and $\Delta S°$, values of $\ln(K_C)$ versus $1/T$ are drawn in a graph. Then, the $\Delta H°$ and the $\Delta S°$ are calculated based on the slope and intercept of the graph and Equation (15) (Vuković *et al.* 2010).

$$\ln K_C = -\frac{\Delta H°}{RT} + \frac{\Delta S°}{R} \tag{15}$$

RESULTS AND DISCUSSION

FTIR, SEM, BET, and zeta potential analyses

Figure 1 represents the FTIR spectra of (a) clinoptilolite, (b) HDTMA-Clino, and (c) NaOH-HDTMA-Clino in a wavenumber range of 4,000–400 cm^{-1}. For clinoptilolite, a wide peak was present in 3,436 cm^{-1} which was related to the stretching vibrations in the bonds of the H_2O molecules in the adsorbent. In 1,633 cm^{-1}, the peak indicated the bending vibrations of H_2O molecules. At 1,162 cm^{-1}, the peaks were representative of stretching of the internal Si–O(Si) and Si–O(Al) vibrations in tetrahedra or alumino– and silico–oxygen bridges. This peak has moved to a slightly higher wavenumber (1,197 and 1,193 cm^{-1}) for HDTMA-Clino and NaOH-HDTMA-Clino because of the loss of some Al^{3+} cations after modification (Mozgawa 2000). The
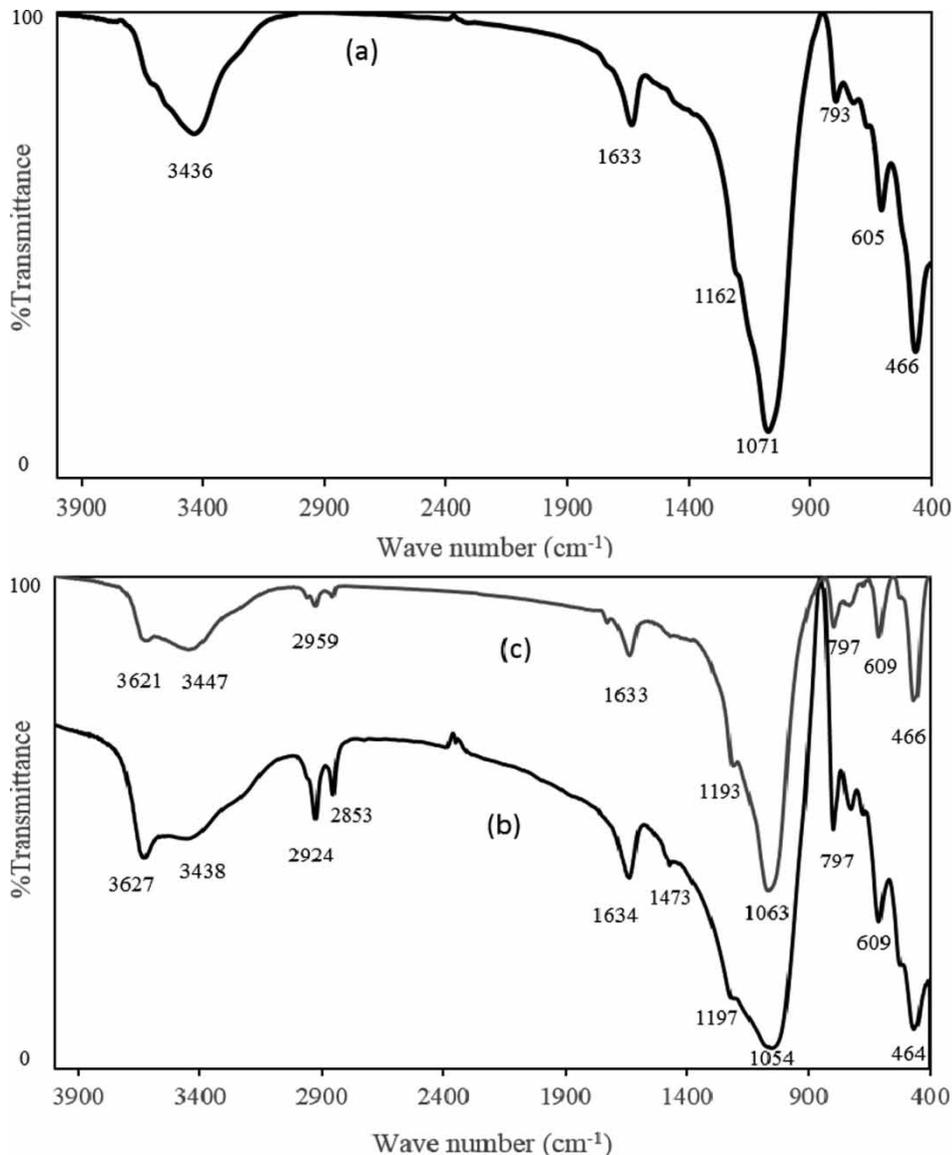
Figure 1 | FTIR spectrum for (a) clinoptilolite, (b) HDTMA-Clino, and (c) NaOH-HDTMA-Clino.

stretching vibrations of T–O in TO_4 (T = Si or Al) appeared in 1,071 cm^{-1}. In 793 cm^{-1}, quartz impurity was present in the FTIR spectrum and in 605 cm^{-1}, the bending vibrations of Si–O–Si or Si–O–Al can be seen. The peak in 466 cm^{-1} showed the bending vibrations of Si–O or Al–O inner bonds.

The peaks that appeared in the FTIR spectrum of clinoptilolite were present in the HDTMA-Clino FTIR spectrum with slight displacements. Also, new peaks appeared in the HDTMA-Clino FTIR spectrum. In 3,627 cm^{-1}, the peak demonstrated the stretching vibrations

of the hydroxyl functional group of the loaded HDTMA surfactant. Another peak appeared at 2,924 cm^{-1}, which displayed the symmetric and asymmetric C–C or C–H bonds in the alkyl chain of the surfactant. This functional group accompanies the adsorption of DCF because of the hydrophobic interactions between the alkyl chain and DCF. Similar results were reported in the literature (Ikhtiyarova *et al.* 2012; Krajišnik *et al.* 2013; Sun *et al.* 2017a, 2017b). The band at 2,853 cm^{-1} introduced symmetric and asymmetric C–H stretching vibrations of the methylene

group of HDTMA. There was also a negligible peak at $1,473\ cm^{-1}$ which was assigned to the asymmetric bending state of the quaternary ammonium of the head methyl group of HDTMA (Aroke & El-Nafaty 2014).

The peaks displayed in HDTMA-Clino occurred in the NaOH-HDTMA-Clino spectrum with slight displacements. Also, the $3,621\ cm^{-1}$ bonds were attributed to the stretching vibrations of the hydroxyl group of the loaded surfactant. The peaks were more intense in clinoptilolite and HDTMA-Clino FTIR spectra than in the one for NaOH-HDTMA-Clino. The decrease in the peak intensities can be due to the decrease in the crystalline characteristic after the alkaline pretreatment (Ates & Akgül 2016).

Figure 2 shows the SEM images of (a) clinoptilolite, (b) HDTMA-Clino before DCF adsorption, (c) HDTMA-Clino after DCF adsorption, (d) NaOH-HDTMA-Clino before DCF adsorption, and (e) NaOH-HDTMA-Clino after DCF adsorption; all with 10,000× magnitude at 2 μm scale. The porous structure of clinoptilolite is obvious in Figure 2(a). After the modification with HDTMA, the surface of clinoptilolite seemed to become less heterogeneous. After the alkaline pretreatment with NaOH, the adsorbent showed a slight hierarchical structure. No obvious differences were observed between the SEM images of the modified adsorbents before and after DCF uptake. This can be due to the absence of any chemical reactions after DCF sorption on both adsorbents.

The BET method was used to determine the specific surface area of clinoptilolite before and after modification. The N_2 adsorption–desorption isotherms at 77 K fitted type IV of the N_2 isotherms which implied the presence of micropores and mesopores in the adsorbent structure. The BET surface area of clinoptilolite was $14.679\ m^2/g$, for HDTMA-Clino, it was $7.329\ m^2/g$, and for NaOH-HDTMA-Clino, the surface area was $10.551\ m^2/g$. The smaller surface area of HDTMA-Clino compared with raw clinoptilolite represented the aggregation of the surfactant molecules on the adsorbent. The total pore volume of clinoptilolite, HDTMA-Clino, and NaOH-HDTMA-Clino was 1.154×10^{-1}, 0.861×10^{-1}, and $1.221 \times 10^{-1}\ cm^3/g$, respectively. The greatest pore volume belonged to the adsorbent modified with alkaline pretreatment. Also, the mean pore volume increased from 315 Å for clinoptilolite to 463 Å for NaOH-HDTMA-Clino.

The zeta potential of the adsorbent represents its surface charge, and it changes after the adsorbent modification with a surfactant and also with the amount of the loaded surfactant (Alkan *et al.* 2005). The zeta potential of clinoptilolite, HDTMA-Clino, and NaOH-HDTMA-Clino were −37, +24.5, and +26.4 mV. The zeta potential of clinoptilolite changed from negative to positive after the modification with HDTMA, indicating the successful loading of the surfactant on the adsorbent surface. Also, the greater positive amount of the zeta potential for NaOH-HDTMA-Clino confirmed the successful loading of more HDTMA molecules on the adsorbent via better accessibility after alkaline pretreatment.

In this research, the experiments showed that after a certain fold of the CMC of the HDTMA solution, further HDTMA loading on clinoptilolite was not possible, unless the surface of the zeolite was modified so that more active sites would be present for the HDTMA molecules to reach. A suitable surface modification was alkaline pretreatment. While the modification of clinoptilolite with HDTMA provided a positive-surface adsorbent, alkaline pretreatment prepared more available adsorption sites for more HDTMA loaded molecules. This way, a more effective adsorbent was prepared under the same conditions. The removal percent and the adsorption capacity comparisons (results are not shown) of the modified clinoptilolite with different amounts of HDTMA showed no significant enhancement after 15× CMC of the loaded HDTMA, but for the alkaline-pretreated clinoptilolite, HDTMA loading was increased to 25 × CMC and the prepared adsorbent was slightly more effective in DCF adsorption. Thus, the HDTMA-Clino was modified at 15 × CMC and NaOH-HDTMA-Clino was modified at 25 × CMC and these adsorbents were used in the experiments.

Contact time experiments

To find the equilibrium contact time for DCF adsorption with HDTMA-Clino and NaOH-HDTMA-Clino, the removal percent and the adsorption capacity were calculated at different contact times for three different initial concentrations. For HDTMA-Clino and NaOH-HDTMA-Clino, the removal percent and the adsorption capacity with 0.5 g adsorbent in 100 mL DCF solutions with 20, 50,
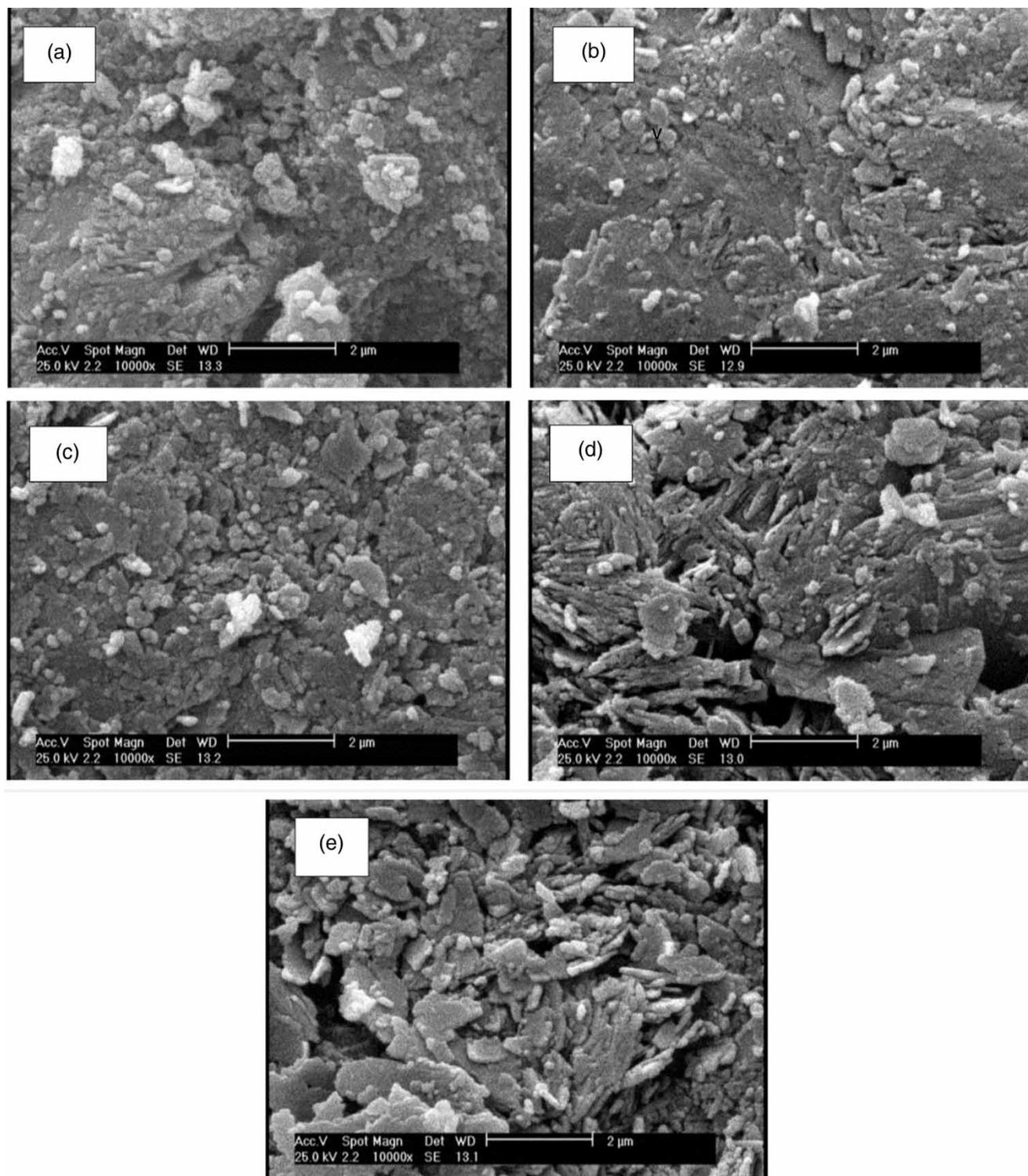
Figure 2 | SEM images of (a) clinoptilolite, (b) HDTMA-Clino before DCF sorption, (c) HDTMA-Clino after DCF sorption, (d) NaOH-HDTMA-Clino before DCF sorption, and (e) NaOH-HDTMA-Clino after DCF sorption; all with 10,000× magnitude at 2 μm scale.

and 80 mg/L concentrations and the contact times of 5, 10, 20, 30, 45, 60, 90, 120, and 180 min were studied.

Figure 3 shows the effect of contact time on (a) DCF removal percent with HDTMA-Clino, (b) DCF adsorption capacity with HDTMA-Clino, (c) DCF removal percent with NaOH-HDTMA-Clino, and (d) DCF adsorption capacity with NaOH-HDTMA-Clino; at three initial concentrations (20, 50, and 80 mg/L), with 0.5 g adsorbent. In the beginning, the adsorption rate was faster and it followed a slighter trend until it became almost steady when the system reached equilibrium. When the adsorption rate does not have significant changes with time, the system has reached equilibrium and that time is considered as the 'equilibrium time'. The rapid changes in the removal percent and the adsorption capacity at the beginning are due to the greater driving force. Also, the presence of more functional groups indicates more available active sites which results in more DCF adsorption (Larous & Meniai 2016). For a 20 mg/L DCF solution, the removal percent with HDTMA-Clino was 91.56% after 90 min. Then, as the contact time increased, only slight changes occurred in the removal percent. A similar trend was obtained for a 50 mg/L DCF solution. For 90 min of contact time, HDTMA-Clino removed 68.00% of DCF from the solution. For an 80 mg/L DCF solution, the removal percent was 53.16% after 90 min. The adsorption capacity also followed an ascending trend for 20, 50, and 80 mg/L DCF solutions by increasing the contact time. Also, the adsorption capacity was higher for greater DCF initial concentrations.

The removal percent diagram for NaOH-HDTMA-Clino followed a similar trend as the one for HDTMA-Clino did. For a 20 mg/L initial concentration, the removal percent of DCF increased by time until it reached 96.94% at 120 min which was not significantly different from 93.61% after 60 min. For a 50 mg/L DCF solution, the removal percent was 91.64% after 60 min. For further increases in the contact time, no significant changes occurred in the removal percent. At an 80 mg/L initial concentration, the removal percent reached 67.89% after 60 min. In greater contact times, the increase in the removal percent was negligible. The adsorption capacity also showed an ascending trend with contact time. For a 20 mg/L DCF solution, the
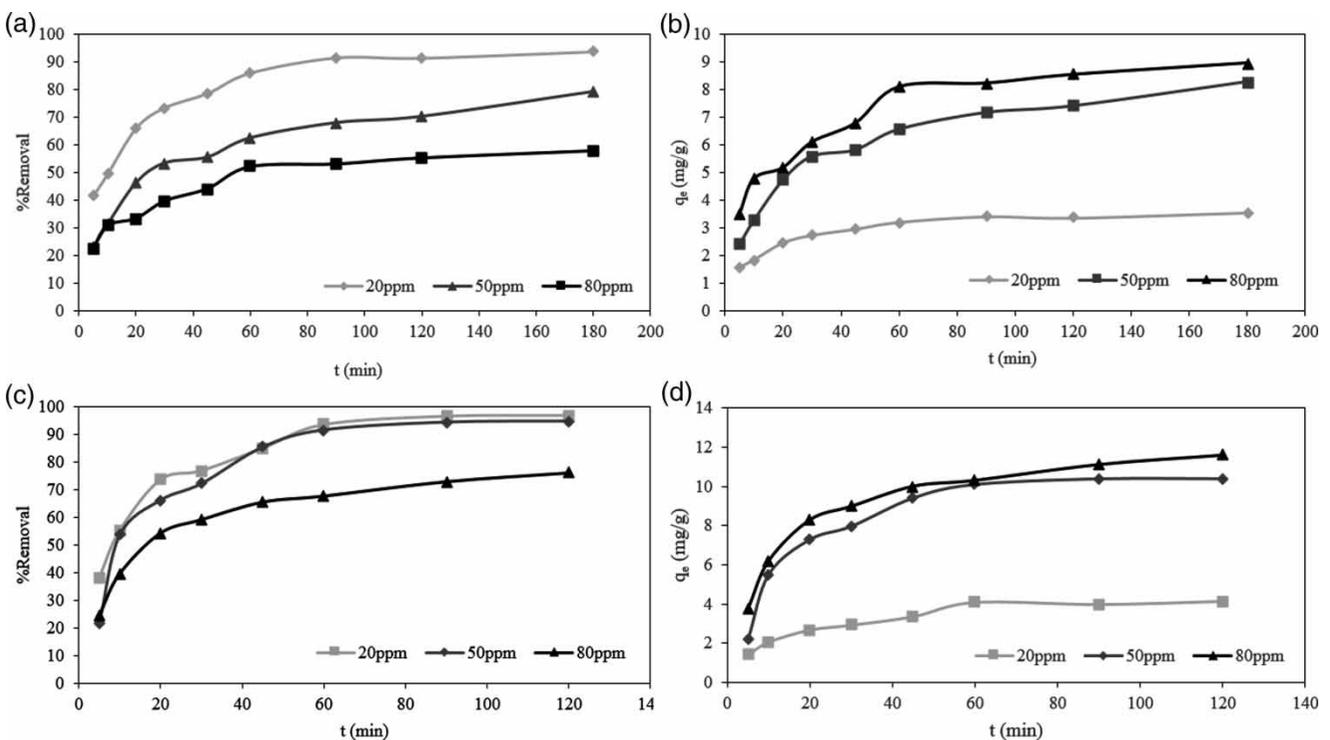

Figure 3 | Effect of contact time on (a) DCF removal percent with HDTMA-Clino, (b) DCF adsorption capacity with HDTMA-Clino, (c) DCF removal percent with NaOH-HDTMA-Clino, and (d) DCF adsorption capacity with NaOH-HDTMA-Clino; at three initial concentrations (20, 50, and 80 mg/L), with 0.5 g adsorbent.

adsorption capacity was 4.15 mg/g at 120 min. The adsorption capacity for a 50 mg/L DCF solution was 10.40 mg/g after 120 min. For a DCF solution with 80 mg/L initial concentration, the adsorption capacity reached 11.59 mg/g at 120 min.

These results showed that the equilibrium contact time was 90 min for HDTMA-Clino and 60 min for NaOH-HDTMA-Clino. So, the alkaline pretreatment was effective in this way and it enhanced the adsorption equilibrium time. The other experiments were later done at these contact periods.

Effect of pH

When the pH of the solution is less than the pK_a (K_a = acid dissociation constant) of DCF, its solubility in the aqueous solution decreases and it starts to precipitate in the solution. First, the pK_a of DCF was investigated and results showed that in pH < 5, DCF starts to precipitate. So, the effect of pH on the adsorption was investigated in the range of 5–10. Figure 4 demonstrates the effect of pH on (a) DCF removal percent and (b) DCF adsorption capacity with HDTMA-Clino and NaOH-HDTMA-Clino; for a 50 mg/L
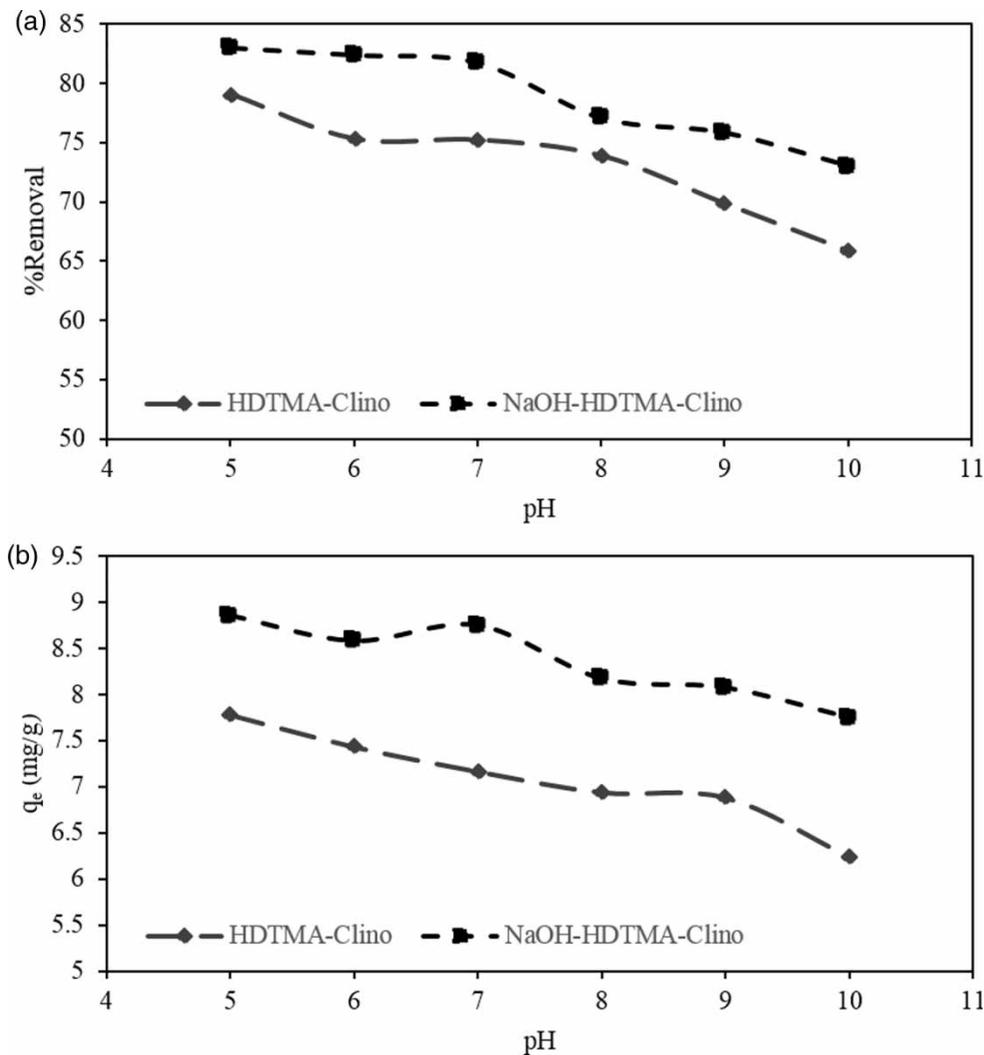

Figure 4 | Effect of pH on (a) DCF removal percent and (b) DCF adsorption capacity with HDTMA-Clino and NaOH-HDTMA-Clino; for a 50 mg/L DCF solution, 0.5 g adsorbent in 100 mL solution, and at the equilibrium contact time.

DCF solution, 0.5 g adsorbent in 100 mL solution, and at the equilibrium contact time. When the solution pH increased from 5 to 7, the removal percent for HDTMA-Clino decreased from 79.05 to 75.23% and the removal percent for NaOH-HDTMA-Clino decreased from 83.01 to 81.74%. A further increase in pH from 7 to 8 made the removal percent for both adsorbents decrease and reach 77.04 and 73.90% for NaOH-HDMA-Clino and HDTMA-Clino, respectively. When the solution pH was equal to 9, NaOH-HDTMA-Clino showed 75.80% and HDTMA-Clino showed 69.87% DCF removal from the solution. Increasing the solution pH to 10 harmed DCF removal for both adsorbents. By increasing the solution pH, the DCF adsorption capacity with both adsorbents decreased. The maximum adsorption capacity for NaOH-HDTMA-Clino was 8.86 mg/g at pH = 5, and the minimum adsorption capacity was 7.75 mg/g in pH = 10. The maximum adsorption capacity for HDTMA-Clino was 7.77 mg/g at pH = 5, and the minimum adsorption capacity was 6.23 mg/g at pH = 10. When the solution pH is more than the pK_a, DCF is present in its anionic form and also its solubility in water increases, so it has a low affinity toward the adsorbent. This results in lower DCF removal percent and adsorption capacity at greater amounts of pH. Besides, increasing the solution pH adds to the number of OH^- groups present in the solution. These OH^- anions hinder the DCF^- anions from reaching the adsorbent surface. The alkaline pretreatment was effective from this point of view because the adsorption capacity and the removal percent were greater for NaOH-HDTMA-Clino than HDTMA-Clino at each pH value.

The remaining bromide anions after the modification of clinoptilolite with HDTMA-Br, which are still present near the positive head of the loaded $HDTMA^+$, leave their place in an anion exchange with DCF^-. Few numbers of DCF^- anions show an affinity for the hydrophobic tails of the loaded HDTMA. The majority of DCF^- anions tend toward the positive head of the loaded HDTMA and are adsorbed on the modified clinoptilolite because of the electrostatic interactions. Because the alkaline pretreatment provides more available active sites through mesopore formation and more exchangeable Na^+ cations on the surface of the adsorbent for HDTMA (so greater amounts of HDTMA can be loaded on the surface of the clinoptilolite),

the adsorption of DCF with NaOH-HDTMA-Clino follows a similar mechanism as with HDTMA-Clino.

Effect of the adsorbent amount

Figure 5 shows the effect of the adsorbent amount on (a) DCF removal percent and (b) DCF adsorption capacity with HDTMA-Clino and NaOH-HDTMA-Clino; for a 50 mg/L DCF solution, at pH = 5, and at the equilibrium contact time. DCF removal percent increased from 83.01 to 97.40% for NaOH-HDTMA-Clino and from 79.05 to 96.17% for HDTMA-Clino when the adsorbent amount increased from 0.5 to 1 g. By further increasing the adsorbent amount from 1 to 2 g, no significant changes occurred in the removal percent. So, 1 g was chosen as the optimum amount for both adsorbents. The increase in the adsorbent amount to 1 g caused the adsorption capacity to decrease to 5.23 mg/g for NaOH-HDTMA-Clino and 4.75 mg/g for HDTMA-Clino. The adsorption capacity followed a decreasing trend by further increases in the adsorbent amount. This trend was because of two reasons: Firstly, in a specific solution concentration and volume, some of the adsorption sites are not involved by increasing the adsorbent amount. Secondly, the aggregation of the adsorbent in greater amounts hinders the accessibility of the adsorption sites for the adsorbate (Lu *et al.* 2016). The greater removal percent and adsorption capacity for NaOH-HDTMA-Clino compared with HDTMA-Clino suggested a more effective DCF adsorption.

Effect of the initial concentration

Figure 6 shows the effect of the initial concentration on DCF adsorption with HDTMA-Clino and NaOH-HDTMA-Clino at (a) 25, (b) 35, and (c) 45 °C, at pH = 5, and 1 g adsorbent. The effect of DCF initial concentration was studied in a range of 20–80 mg/L. At 25 °C, the removal percent of a 20 mg/L DCF solution with HDTMA-Clino was 96.62% and it was 98.67% with NaOH-HDTMA-Clino. The removal percent then followed a decreasing trend for both adsorbents in greater initial concentrations. At 35 °C, the maximum removal percent also occurred for a 20 mg/L DCF solution which was 96.35% for HDTMA-Clino and 97.83% for NaOH-HDTMA-Clino. At 45 °C, like the other
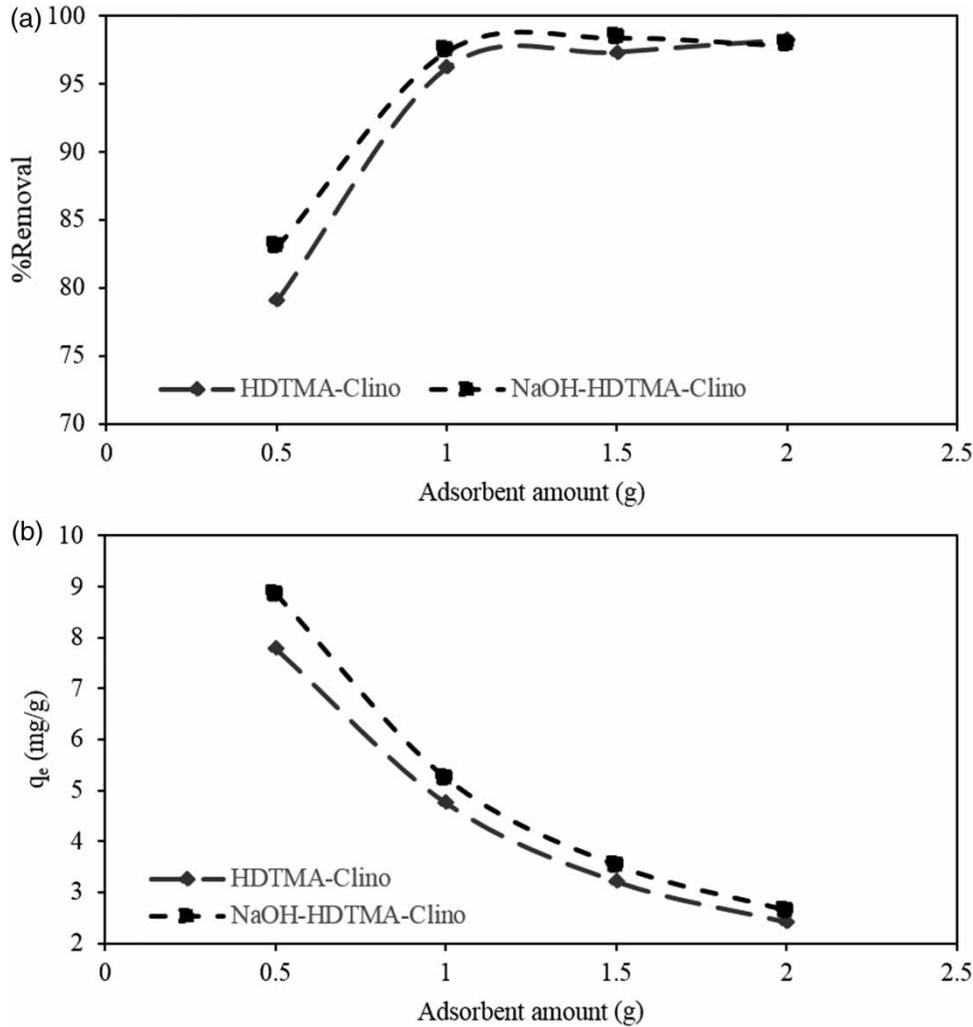
Figure 5 │ Effect of the adsorbent amount on (a) DCF removal percent and (b) DCF adsorption capacity with HDTMA-Clino and NaOH-HDTMA-Clino; for a 50 mg/L DCF solution, at pH = 5, and at the equilibrium contact time.

two temperatures, the highest removal percent occurred for a 20 mg/L initial concentration, which was 97.70% for NaOH-HDTMA-Clino; about 2.25% more than that for HDTMA-Clino. At 25 °C and for a 20 mg/L DCF solution, the adsorption capacity was 1.77 mg/g for HDTMA-Clino and 1.97 mg/g for NaOH-HDTMA-Clino. Then, the adsorption capacity increased as the initial concentration increased. Similarly, at 35 °C, an ascending trend in the adsorption capacity was observed. For a 20 mg/L DCF solution, the minimum adsorption capacity was 1.82 mg/g with HDTMA-Clino and 1.99 mg/g with NaOH-HDTMA-Clino. At 45 °C, the adsorption capacity was 1.82 mg/g for HDTMA-Clino and 2.02 mg/g for NaOH-HDTMA-Clino. In addition to the ascending trend of the adsorption capacity and the descending trend of the removal percent with the initial concentration at each temperature, NaOH-HDTMA-Clino showed better removal efficiency than HDTMA-Clino.

The decrease in the removal percent with increasing the initial concentration was because of the saturation of the finite adsorption sites in a specific adsorbent amount (Meitei & Prasad 2014). The increasing trend of the adsorption capacity with the initial concentration was due to a greater concentration difference between the solid–liquid phase which itself caused a greater driving force (Zeng *et al.* 2010).
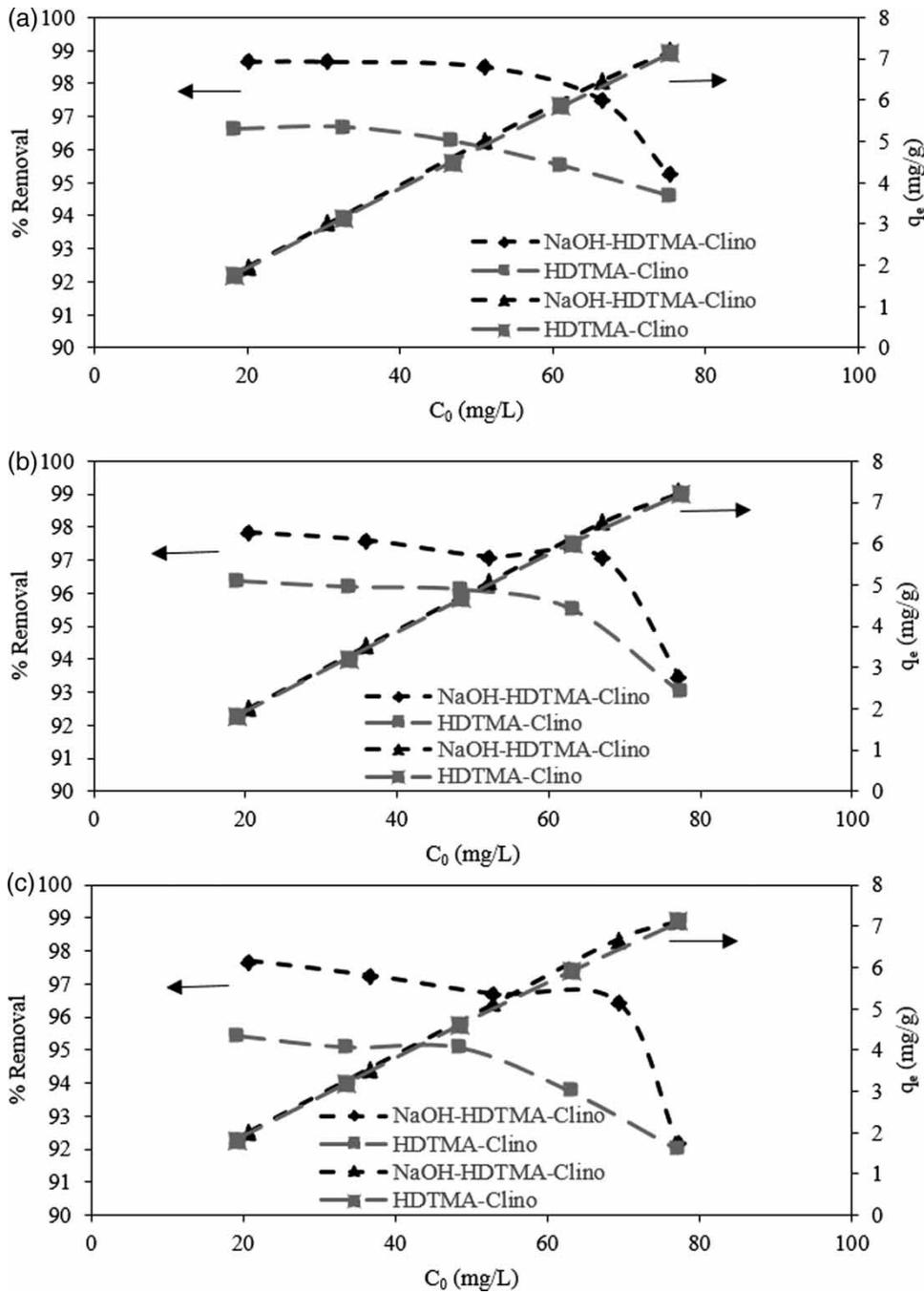
Figure 6 | Effect of the initial concentration on DCF adsorption with HDTMA-Clino and NaOH-HDTMA-Clino at (a) 25, (b) 35, and (c) 45 °C; at pH = 5, and 1 g adsorbent.

Effect of the temperature

The effect of the temperature was studied at 25, 35, and 45 °C. At 25 °C, HDTMA-Clino showed 96.62% DCF removal and NaOH-HDTMA-Clino removed 98.67% of DCF from a 20 mg/L DCF solution. At 35 °C, DCF removal

percent with both adsorbents decreased slightly, and for a DCF solution with 20 mg/L concentration, it reached 96.35% with HDTMA-Clino and 97.83% with NaOH-HDTMA-Clino. The descending trend continued, and DCF removal percent for a 20 mg/L DCF solution was 95.45% for HDTMA-Clino and 97.70% for NaOH-HDTMA-Clino.

So, the removal percent with both adsorbents decreased slightly and almost negligibly by increasing the temperature. DCF adsorption capacity with both adsorbents for each initial concentration remained almost the same with temperature changes. This showed that temperature had an adverse, although not considerable, effect on the adsorption and that the process was exothermic. So, 25 °C was a more suitable temperature than 35 and 45 °C.

Isotherm study

Relevant parameters of the isotherm models are represented in Tables 1 and 2. For DCF adsorption with HDTMA-Clino, the R^2 value of the Temkin isotherm model was 9.972×10^{-1} at 25 °C, 9.854×10^{-1} at 35 °C, and 9.939×10^{-1} at 45 °C. These R^2 values were greater than the R^2 values of the other isotherm models. Also, the root-mean-squared error (RMSE) value for Temkin isotherm was 9.950×10^{-1} at 25 °C, 2.312×10^{-1} at 35 °C, and 1.467×10^{-1} at 45 °C. These RMSE values were the least among all the others at each temperature. Thus, for DCF adsorption with HDTMA-Clino, the Temkin isotherm model fitted the experimental data best.

Table 1 | Isotherm parameters of Langmuir, Freundlich, Temkin, and D-R models for DCF adsorption with HDTMA-Clino

Isotherm model	Parameters	298.15 K	308.15 K	318.15 K
Langmuir	$q_{m,cal}$ (mg/g) $\times 10^{-1}$	1.46843	1.22100	1.31752
	K_L (L/mg) $\times 10$	2.396	2.893	1.992
	$R^2 \times 10$	9.702	9.460	9.656
	RMSE $\times 10$	1.224	3.153	1.995
Freundlich	K_F (mg/g)	2.7568	2.6479	2.1953
	n	1.3626	1.4712	1.4278
	$(1/n) \times 10$	7.339	6.797	7.004
	$R^2 \times 10$	9.780	9.434	9.680
	RMSE $\times 10$	3.265	6.552	4.405
Temkin	β	2.8498	2.7214	2.7522
	K_T (L/g)	2.8829	2.8133	2.1427
	$R^2 \times 10$	9.972	9.854	9.939
	RMSE $\times 10$	0.995	2.312	1.467
D-R	q_D (mg/g)	6.7248	6.7517	6.4689
	K $(mol^2/J^2) \times 10^7$	2	3	3
	E (kJ/mol)	1.5811	1.2910	1.2910
	$R^2 \times 10$	9.659	9.568	9.426
	RMSE $\times 10$	6.297	4.656	5.873

Table 2 | Isotherm parameters of Langmuir, Freundlich, Temkin, and D-R models for DCF adsorption with NaOH-HDTMA-Clino

Isotherm model	Parameters	298.15 K	308.15 K	318.15 K
Langmuir	$q_{m,cal}$ (mg/g) $\times 10^{-1}$	1.10132	1.76991	1.47711
	K_L (L/mg) $\times 10$	9.190	2.834	3.216
	$R^2 \times 10$	9.540	9.385	9.706
	RMSE $\times 10$	2.817	1.560	1.337
Freundlich	K_F (mg/g)	5.1689	3.8054	3.4794
	n	1.5375	1.2868	1.3862
	$(1/n) \times 10$	6.504	7.771	7.214
	$R^2 \times 10$	9.464	9.966	9.99
	RMSE $\times 10$	5.055	1.165	0.591
Temkin	β	2.522	2.9088	2.7608
	K_T (L/g)	8.4659	4.2061	4.0314
	$R^2 \times 10$	9.868	9.701	9.721
	RMSE $\times 10$	2.008	2.916	2.899
D-R	q_D (mg/g)	7.2725	6.7013	6.4876
	K $(mol^2/J^2) \times 10^7$	0.9	1.0	1.0
	E (kJ/mol)	2.3570	2.2361	2.2361
	$R^2 \times 10$	9.969	9.579	9.436
	RMSE $\times 10$	0.870	7.375	7.608

For DCF adsorption with NaOH-HDTMA-Clino, at 25 °C, the R^2 value for D–R isotherm was 9.969×10^{-1}, which was the greatest compared with the R^2 values of other isotherm models at 25 °C. The calculated RMSE for D–R isotherm at 25 °C was 8.700×10^{-2}, which was the least compared with the RMSE values of other models at the same temperature. The R^2 value for the Freundlich isotherm model was 9.966×10^{-1} at 35 °C and 9.990×10^{-1} at 45 °C. These R^2 values were closer to unity than the R^2 values of other isotherms at 35 and 45 °C. So, D–R isotherm at 25 °C and Freundlich isotherm at 35 and 45 °C were in best agreement with the experimental data.

The R_L values were between 0 and 1 for all the studied concentrations. This indicated that for the adsorption of DCF from an aqueous solution, HDTMA-Clino and NaOH-HDTMA-Clino were both effective adsorbents. The maximum adsorption capacity predicted by the Langmuir model was 14.6843 mg/g at 25 °C with HDTMA-Clino and 17.6991 mg/g at 35 °C with NaOH-HDTMA-Clino. For DCF adsorption with both adsorbents, *n* was greater than 1 which confirmed a physisorption. For HDTMA-Clino, K_T decreased from 2.8829 to 2.1427 L/g as the temperature increased from 25 to 45 °C. This was related to weaker bonds between DCF and the adsorbent at 45 °C. The

Table 3 │ Kinetic parameters for DCF adsorption with HDTMA-Clino; at three different initial concentrations

Kinetic model	Parameters	20 mg/L	50 mg/L	80 mg/L
Pseudo first order	K_1 $(min^{-1}) \times 10^2$	3.86	3.54	5.65
	$q_{e,cal}$ (mg/g)	2.2298	5.3527	8.1328
	$R^2 \times 10$	9.901	9.705	8.215
	RMSE	1.1834	1.8114	0.8932
Pseudo second order	K_2 (g/(mg min)) $\times 10^2$	2.76	0.61	0.77
	$q_{e,cal}$ (mg/g)	3.7175	8.8496	9.5420
	$R^2 \times 10$	9.990	9.953	9.965
	RMSE $\times 10$	1.166	2.876	5.027
Intraparticle diffusion	$K_{id,1}$ $(mg/(g\ min^{0.5})) \times 10$	3.021	7.455	7.607
	c (mg/g)	0.9626	1.0392	1.9589
	$R^2 \times 10$	9.733	9.563	9.715
	RMSE $\times 10$	0.957	3.050	2.494
	$K_{id,3}$ $(mg/(g\ min^{0.5})) \times 10$	0.403	2.897	1.836
	c (mg/g)	2.9896	4.3538	6.5004
	$R^2 \times 10$	6.520	9.710	9.963
	RMSE $\times 10$	4.768	0.812	0.182

β parameter is related to the adsorption heat, and it decreased from 2.8498 to 2.7522 as the temperature increased from 25 to 45 °C. DCF adsorption with both adsorbents was physical because the E values were all less than 8 kJ/mol, so the interactions between DCF and the adsorbent were mainly due to Van der Waals forces, and the adsorption process was reversible. This was commensurate with the temperature study which revealed that 25 °C was more suitable than 35 and 45 °C.

Kinetic study

Table 3 shows the kinetic parameters of DCF adsorption with HDTMA-Clino, and Table 4 represents the same data for NaOH-HDTMA-Clino. The R^2 values of DCF adsorption with HDTMA-Clino at 20, 50, and 80 mg/L initial concentrations were the highest for the pseudo-second-order kinetic model. Thus, the adsorption followed the pseudo-second-order model. According to this model, the occupation of the adsorption sites is proportionate to the square of the number of these sites and the process is a physisorption (Ren et al. 2016). For DCF adsorption with NaOH-HDTMA-Clino with DCF solutions at 20, 50, and 80 mg/L concentrations, the R^2 values for the pseudo-second-order kinetic model were 9.942×10^{-1}, 9.913×10^{-1}, and 9.993×10^{-1}, which were greater than the R^2 values of the pseudo-first-order kinetic model. Hence, the kinetic of DCF adsorption with both adsorbents was in better agreement with the pseudo-second-order model.

Table 4 │ Kinetic parameters for DCF adsorption with NaOH-HDTMA-Clino; at three different initial concentrations

Kinetic model	Parameters	20 mg/L	50 mg/L	80 mg/L
Pseudo first order	K_1 $(min^{-1}) \times 10^2$	3.10	5.62	7.32
	$q_{e,cal}$ (mg/g)	2.8953	9.3962	9.2748
	$R^2 \times 10$	9.821	9.727	9.838
	RMSE	1.1940	0.8680	1.0760
Pseudo second order	K_2 (g/(mg min)) $\times 10^2$	1.58	0.57	0.70
	$q_{e,cal}$ (mg/g)	4.6253	11.9761	12.5786
	$R^2 \times 10$	9.942	9.913	9.993
	RMSE $\times 10$	1.769	4.676	1.929
Intraparticle diffusion	$K_{id,1}$ $(mg/(g\ min^{0.5}))$	0.702	3.5785	2.6477
	c (mg/g)	-0.1704	-5.804	-2.1677
	R^2	1	1	1
	RMSE $\times 10^4$	0	2	1
	$K_{id,2}$ $(mg/(g\ min^{0.5})) \times 10$	3.084	9.566	7.673
	c (mg/g)	1.2700	2.9122	4.8276
	$R^2 \times 10$	9.898	9.776	9.969
	RMSE $\times 10$	0.286	1.325	0.392
	$K_{id,3}$ $(mg/(g\ min^{0.5})) \times 10$	0.152	0.948	4.028
	c (mg/g)	3.9325	9.4110	7.2167
	$R^2 \times 10$	8.760	8.080	9.909
	RMSE $\times 10^2$	6.43	6.06	5.07

Table 5 | Thermodynamic parameters of DCF adsorption with HDTMA-Clino and NaOH-HDTMA-Clino

Adsorbent	T (K)	K$_C$	ΔG^O (J/mol)	ΔH^O (J/mol)	ΔS^O (J/(mol K))
HDTMA-Clino	298.15	1.3035	-6.5702×10^2	-9.91361×10^3	-3.07493×10
	308.15	1.2777	-6.2784×10^2		
	318.15	1.0113	-2.9720×10		
NaOH-HDTMA-Clino	298.15	2.3578	-2.12615×10^3	-1.48546×10^4	-4.31397×10
	308.15	1.6445	-1.27441×10^3		
	318.15	1.6236	-1.28194×10^3		

Figure 7 shows the different stages of DCF adsorption with HDTMA-Clino and NaOH-HDTMA-Clino according to the intraparticle diffusion model at 20, 50, and 80 mg/L initial concentration. According to this kinetic model, the first stage is for the external adsorption on the adsorbent surface, the second stage, which occurs with a slighter slope, is the gradual diffusion of the adsorbate into the adsorbent, and the third slower and more constant stage is the equilibrium of the adsorbate in the active sites of the adsorbent. For NaOH-HDTMA-Clino, all the three stages were obvious and separable compared with the results for HDTMA-Clino because more surface area was reachable for DCF anions through mesopore formation after the alkaline pretreatment (Benkli *et al.* 2005; Jia *et al.* 2017).

The boundary layer effect was also investigated through the calculation of the *c* parameter (intercept of the intraparticle diffusion model, before dividing it to several stages). For both adsorbents, the adjusted line of the intraparticle diffusion model did not cross the zero point of the coordinates, so the adsorption happened at different stages. For DCF adsorption with HDTMA-Clino, at 20, 50, and 80 mg/L, the *c* parameter was 1.5422, 2.1517, and 3.2015 mg/g, respectively, and for NaOH-HDTMA-Clino, the related *c* values were 1.092, 2.5386, and 3.6674 mg/g. This indicated that at greater initial concentrations, the adsorption was mostly affected by the boundary layer and that the intraparticle diffusion was not the sole present mechanism in the process.

Thermodynamic study

Table 5 shows the thermodynamic parameters of DCF adsorption with HDTMA-Clino and NaOH-HDTMA-Clino at 25, 35, and 45 °C. K_C, $\Delta G°$, $\Delta H°$, and $\Delta S°$ at these three temperatures

were calculated according to Equations (14) and (15). For DCF adsorption with both adsorbents, $\Delta G°$ was negative at these three temperatures which showed spontaneous adsorption. Also, at 25 °C, $\Delta G°$ was more negative than at the other two temperatures; thus, 25 °C favored the adsorption more than 35 and 45 °C. The negative amount of $\Delta H°$ indicated exothermic DCF adsorption with both adsorbents. The standard enthalpy change between 2 and 21 kJ/mol shows physisorption, while its changes between 80 and 200 kJ/mol indicate chemisorption (Vuković *et al.* 2010). The $|\Delta H°|$ for DCF adsorption with HDTMA-Clino and NaOH-HDTMA-Clino was 9.913 and 14.85 kJ/mol, respectively. These results confirmed the physisorption and agreed with the results obtained from the isotherm and kinetic studies. The negative value of $\Delta S°$

Table 6 | Comparison of the equilibrium contact time and maximum DCF adsorption capacity for different adsorbents

| Adsorbent	t$_e$ (min)	q$_m$ (mg/g)	Reference
Graphene oxide	1440	5.00×10^2	(Nam, Jung *et al.* 2015)
ZSM-5 zeolite	60	1.53×10^2	(Rac, Rakić *et al.* 2020)
Grape bagasse	1400	7.698×10	(Antunes, Esteves *et al.* 2012)
Zeolite modified with CPC	-	4.726×10	(Krajišnik, Daković *et al.* 2011)
Zeolite modified with CTAB	120	4.294×10	(Sun, Shi *et al.* 2017)
NaOH-HDTMA-Clino	60	1.769×10	present study
HDTMA-Clino	90	1.468×10	present study
Activated carbon from olive stones	30	1.100×10	(Larous, and Meniai 2016)
Activated carbon from coca pod husk	45	4.741×10^{-1}	(de Luna, Murniati *et al.* 2017)
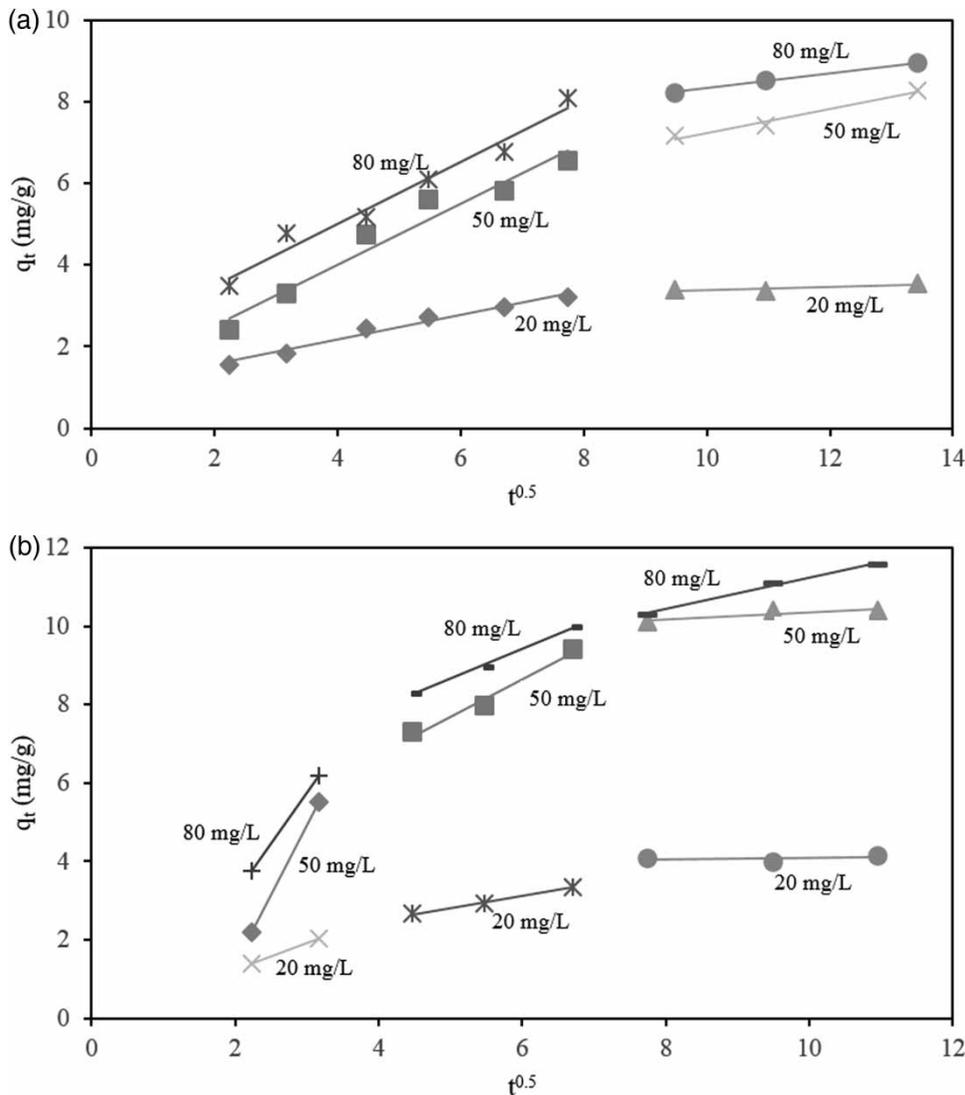
Figure 7 │ Different stages of DCF adsorption with (a) HDTMA-Clino and (b) NaOH-HDTMA-Clino according to the intraparticle diffusion model at 20, 50, and 80 mg/L initial concentration.

shows a decrease in the degree of freedom of the adsorbate ions after the adsorption (Hu *et al.* 2017). The $\Delta S°$ for DCF adsorption with HDTMA-Clino and NaOH-HDTMA-Clino was −30.7493 and −43.1397 J/(mol K), respectively. The negative changes in the standard entropy suggested a decrease in the degree of freedom of DCF anions after the adsorption.

To summarize, clinoptilolite is an abundant and inexpensive natural zeolite, which has shown to be effective in DCF adsorption. It has an inherently negative charge and mostly possesses micropores, thus it was modified with a cationic surfactant to have affinity toward DCF anions. Then, the effect of alkaline pretreatment on the adsorption

was also investigated. The equilibrium contact time for DCF adsorption with both HDTMA-Clino and NaOH-HDTMA-Clino was less than 2 h with more than 90% DCF removal, which was a satisfying result. According to BET analysis, although alkaline pretreatment increased the specific surface area and the total pore volume of HDTMA-Clino, it might not be necessary to apply this pretreatment at these concentrations of DCF under these sets of conditions; as the HDTMA-Clino itself adsorbed more than 90% of DCF from the solution and its DCF adsorption capacity improved by a maximum of about 3 mg/g after NaOH pretreatment.

A comparison of the equilibrium contact time and maximum DCF adsorption capacity from the Langmuir model for the different adsorbents from the literature are summarized in Table 6. The studies are ordered based on a descending trend for q_m. One must be wary that any further conclusions based on this table are only valid if the impact of the other adsorption parameters is taken into account, so a thorough study of the literature is suggested before making a final decision.

Future studies can focus on the effectiveness of alkaline pretreatment of clinoptilolite for much greater concentrations of DCF, much smaller amounts of the adsorbent, or DCF adsorption capacity of NaOH-HDTMA-Clino in the presence of other pollutants. Also, the modification of clinoptilolite with other cationic surfactants together with NaOH pretreatment for DCF adsorption can be explored. Enthusiastic researchers might be interested in the life cycle of the adsorbent and a focus on reviving and reusing clinoptilolite in DCF adsorption or for other purposes.

CONCLUSIONS

Clinoptilolite was not effective in DCF adsorption because of its negative surface charge, so it was modified to HDMA-Clino and NaOH-HDTMA-Clino. The zeta potential measurement revealed a positive-surface charge for both modified adsorbents and the BET analysis reported greater total pore volume and mean pore volume for NaOH-HDTMA-Clino. The adsorption equilibrium time with NaOH-HDTMA-Clino was 30 min sooner than HDTMA-Clino. The optimum pH was the least possible pH value before DCF started to dissociate (pH = 5), and the optimum adsorbent amount was 1 g in 100 mL for a 50 mg/L DCF solution. The temperature had a slight adverse effect on DCF adsorption and 25 °C concluded to be better than 35 and 45 °C. The isotherm study stated a heterogeneous surface for the adsorbents. The E parameter amounts at 25, 35, and 45 °C were less than 8 kJ/mol, so the adsorption was physisorption and mainly due to the electrostatic forces. The adsorption was in better agreement with the pseudo-second-order kinetic model, and it was also spontaneous.

Using HDTMA-Clino, the $\Delta H°$ was -9.91361×10^3 J/mol and the $\Delta S°$ was -30.7493 J/(mol K) and with NaOH-HDTMA-Clino, $\Delta H°$ was -1.48546×10^4 J/mol and $\Delta S°$ was -43.1397 J/(mol K). These negative changes implied exothermic adsorption with a decrease in the degree of freedom of DCF anions after adsorption. The NaOH pretreatment had a positive, albeit inconsiderable, effect on HDTMA-Clino for DCF adsorption.

DATA AVAILABILITY STATEMENT

All relevant data are included in the paper or its Supplementary Information.

REFERENCES

Akhtar, J., Amin, N. A. S. & Shahzad, K. 2016 A review on removal of pharmaceuticals from water by adsorption. *Desalination and Water Treatment* **57** (27), 12842–12860. https://doi.org/10.1080/19443994.2015.1051121.

Alkan, M., Tekin, G. & Namli, H. 2005 FTIR and zeta potential measurements of sepiolite treated with some organosilanes. *Microporous and Mesoporous Materials* **84** (1–3), 75–83. https://doi.org/10.1016/j.micromeso.2005.05.016.

Ambrozova, P., Kynicky, J., Urubek, T. & Nguyen, V. 2017 Synthesis and modification of clinoptilolite. *Molecules* **22** (7), 1107. https://doi.org/10.3390/molecules22071107.

Antunes, M., Esteves, V. I., Guégan, R., Crespo, J. S., Fernandes, A. N. & Giovanela, M. 2012 Removal of diclofenac sodium from aqueous solution by Isabel grape bagasse. *Chemical Engineering Journal* **192** (Suppl. C), 114–121. https://doi.org/10.1016/j.cej.2012.03.062.

Aroke, U. & El-Nafaty, U. 2014 XRF, XRD and FTIR properties and characterization of HDTMA-Br surface modified organo-kaolinite clay. *International Journal of Emerging Technology and Advanced Engineering* **4** (4), 817–825.

Ates, A. & Akgül, G. 2016 Modification of natural zeolite with NaOH for removal of manganese in drinking water. *Powder Technology* **287**, 285–291. https://doi.org/10.1016/j.powtec.2015.10.021.

Benkli, Y. E., Can, M. F., Turan, M. & Çelik, M. S. 2005 Modification of organo-zeolite surface for the removal of reactive azo dyes in fixed-bed reactors. *Water Research* **39** (2), 487–493. https://doi.org/10.1016/j.watres.2004.10.008.

Boparai, H. K., Joseph, M. & O'Carroll, D. M. 2011 Kinetics and thermodynamics of cadmium ion removal by adsorption onto nano zerovalent iron particles. *Journal of Hazardous Materials* **186** (1), 458–465. https://doi.org/10.1016/j.jhazmat.2010.11.029.

Cifuentes, A., Bernal, J. L. & Diez-Masa, J. C. 1997 Determination of critical micelle concentration values using capillary electrophoresis instrumentation. *Analytical Chemistry* **69** (20), 4271–4274. https://doi.org/10.1021/ac970696n.

de Luna, M. D. G., Murniati, B. W., Rivera, K. K. P. & Arazo, R. O. 2017 Removal of sodium diclofenac from aqueous solution by adsorbents derived from cocoa pod husks. *Journal of Environmental Chemical Engineering* **5** (2), 1465–1474. https://doi.org/10.1016/j.jece.2017.02.018.

El-Kamash, A. 2008 Evaluation of zeolite A for the sorptive removal of Cs^+ and Sr^{2+} ions from aqueous solutions using batch and fixed bed column operations. *Journal of Hazardous Materials* **151** (2–3), 432–445. https://doi.org/10.1016/j.jhazmat.2007.06.009.

Fallou, H., Cimetière, N., Giraudet, S., Wolbert, D. & Le Cloirec, P. 2016 Adsorption of pharmaceuticals onto activated carbon fiber cloths – modeling and extrapolation of adsorption isotherms at very low concentrations. *Journal of Environmental Management* **166**, 544–555. https://doi.org/10.1016/j.jenvman.2015.10.056.

Hu, X. & Cheng, Z. 2015 Removal of diclofenac from aqueous solution with multi-walled carbon nanotubes modified by nitric acid. *Chinese Journal of Chemical Engineering* **23** (9), 1551–1556. https://doi.org/10.1016/j.cjche.2015.06.010.

Hu, C., Zhu, P., Cai, M., Hu, H. & Fu, Q. 2017 Comparative adsorption of Pb (II), Cu (II) and Cd (II) on chitosan saturated montmorillonite: kinetic, thermodynamic and equilibrium studies. *Applied Clay Science* **143**, 320–326. https://doi.org/10.1016/j.clay.2017.04.005.

Huguet, M., Deborde, M., Papot, S. & Gallard, H. 2013 Oxidative decarboxylation of diclofenac by manganese oxide bed filter. *Water Research* **47** (14), 5400–5408. https://doi.org/10.1016/j.watres.2013.06.016.

Ikhtiyarova, G., Özcan, A., Gök, Ö. & Özcan, A. 2012 Characterization of natural-and organobentonite by XRD, SEM, FTIR and thermal analysis techniques and its adsorption behaviour in aqueous solutions. *Clay Minerals* **47** (1), 31–44. https://doi.org/10.1180/claymin.2012.047.1.31.

Jia, Z., Li, Z., Ni, T. & Li, S. 2017 Adsorption of low-cost absorption materials based on biomass (*Cortaderia selloana* flower spikes) for dye removal: kinetics, isotherms and thermodynamic studies. *Journal of Molecular Liquids* **229**, 285–292. https://doi.org/10.1016/j.molliq.2016.12.059.

Jiménez-Castañeda, M. & Medina, D. 2017 Use of surfactant-modified zeolites and clays for the removal of heavy metals from water. *Water* **9** (4), 235. https://doi.org/10.3390/w9040235.

Khambhaty, Y., Mody, K., Basha, S. & Jha, B. 2009 Kinetics, equilibrium and thermodynamic studies on biosorption of hexavalent chromium by dead fungal biomass of marine *Aspergillus niger*. *Chemical Engineering Journal* **145** (3), 489–495. https://doi.org/10.1016/j.cej.2008.05.002.

Kim, J. S., Lee, Y. Y. & Kim, T. H. 2016 A review on alkaline pretreatment technology for bioconversion of lignocellulosic biomass. *Bioresource Technology* **199**, 42–48. https://doi.org/10.1016/j.biortech.2015.08.085.

Krajišnik, D., Daković, A., Milojević, M., Malenović, A., Kragović, M., Bogdanović, D. B., Dondur, V. & Milić, J. 2011 Properties of diclofenac sodium sorption onto natural zeolite modified with cetylpyridinium chloride. *Colloids and Surfaces B: Biointerfaces* **83** (1), 165–172. https://doi.org/10.1016/j.colsurfb.2010.11.024.

Krajišnik, D., Daković, A., Malenović, A., Djekić, L., Kragović, M., Dobričić, V. & Milić, J. 2013 An investigation of diclofenac sodium release from cetylpyridinium chloride-modified natural zeolite as a pharmaceutical excipient. *Microporous and Mesoporous Materials* **167**, 94–101. https://doi.org/10.1016/j.micromeso.2012.03.033.

Larous, S. & Meniai, A.-H. 2016 Adsorption of diclofenac from aqueous solution using activated carbon prepared from olive stones. *International Journal of Hydrogen Energy* **41** (24), 10380–10390. https://doi.org/10.1016/j.ijhydene.2016.01.096.

Lu, X., Shao, Y., Gao, N., Chen, J., Zhang, Y., Wang, Q. & Lu, Y. 2016 Adsorption and removal of clofibric acid and diclofenac from water with MIEX resin. *Chemosphere* **161**, 400–411. https://doi.org/10.1016/j.chemosphere.2016.07.025.

Meitei, M. D. & Prasad, M. N. V. 2014 Adsorption of Cu (II), Mn (II) and Zn (II) by *Spirodela polyrhiza* (L.) Schleiden: equilibrium, kinetic and thermodynamic studies. *Ecological Engineering* **71**, 308–317. https://doi.org/10.1016/j.ecoleng.2014.07.036.

Misaelides, P. 2011 Application of natural zeolites in environmental remediation: a short review. *Microporous and Mesoporous Materials* **144** (1–3), 15–18. https://doi.org/10.1016/j.micromeso.2011.03.024.

Mozgawa, W. 2000 The influence of some heavy metals cations on the FTIR spectra of zeolites. *Journal of Molecular Structure* **555** (1), 299–304. https://doi.org/10.1016/S0022-2860(00)00613-X.

Nam, S.-W., Jung, C., Li, H., Yu, M., Flora, J. R. V., Boateng, L. K., Her, N., Zoh, K.-D. & Yoon, Y. 2015 Adsorption characteristics of diclofenac and sulfamethoxazole to graphene oxide in aqueous solution. *Chemosphere* **136** (Suppl. C), 20–26. https://doi.org/10.1016/j.chemosphere.2015.03.061.

Poorsharbaf Ghavi, F., Raouf, F. & Dadvand Koohi, A. 2020 A review on diclofenac removal from aqueous solution, emphasizing on adsorption method. *Iranian Journal of Chemistry and Chemical Engineering (IJCCE)* **39** (1), 141–154. https://doi.org/10.30492/ijcce.2020.33337.

Rac, V., Rakić, V., Stošić, D., Pavlović, V., Bosnar, S. & Auroux, A. 2020 Enhanced accessibility of active sites in hierarchical ZSM-5 zeolite for removal of pharmaceutically active substances: adsorption and microcalorimetric study. *Arabian Journal of Chemistry* **13** (1), 1945–1954. https://doi.org/10.1016/j.arabjc.2018.02.012.

Ren, H., Gao, Z., Wu, D., Jiang, J., Sun, Y. & Luo, C. 2016 Efficient Pb(ii) removal using sodium alginate–carboxymethyl cellulose gel beads: preparation, characterization, and adsorption mechanism. *Carbohydrate Polymers*

137, 402–409. https://doi.org/10.1016/j.carbpol.2015. 11.002.

Sotelo, J. L., Ovejero, G., Rodríguez, A., Álvarez, S., Galán, J. & García, J. 2014 Competitive adsorption studies of caffeine and diclofenac aqueous solutions by activated carbon. *Chemical Engineering Journal* **240** (Suppl. C), 443–453. https://doi.org/ 10.1016/j.cej.2013.11.094.

Sun, K., Shi, Y., Chen, H., Wang, X. & Li, Z. 2017a Extending surfactant-modified 2:1 clay minerals for the uptake and removal of diclofenac from water. *Journal of Hazardous Materials* **323**, 567–574. https://doi.org/10.1016/j.jhazmat. 2016.05.038.

Sun, K., Shi, Y., Wang, X. & Li, Z. 2017b Sorption and retention of diclofenac on zeolite in the presence of cationic surfactant. *Journal of Hazardous Materials* **323**, 584–592. https://doi. org/10.1016/j.jhazmat.2016.08.026.

Tran, H. N., Viet, P. V. & Chao, H.-P. 2018 Surfactant modified zeolite as amphiphilic and dual-electronic adsorbent for removal of cationic and oxyanionic metal ions and organic compounds. *Ecotoxicology and Environmental Safety* **147**, 55–63. https://doi.org/10.1016/ j.ecoenv.2017.08.027.

Urum, K. & Pekdemir, T. 2004 Evaluation of biosurfactants for crude oil contaminated soil washing. *Chemosphere* **57** (9), 1139–1150. https://doi.org/10.1016/j.chemosphere.2004.07.048.

Vuković, G. D., Marinković, A. D., Čolić, M., Ristić, M. Đ., Aleksić, R., Perić-Grujić, A. A. & Uskoković, P. S. 2010 Removal of cadmium from aqueous solutions by oxidized and ethylenediamine-functionalized multi-walled carbon nanotubes. *Chemical Engineering Journal* **157** (1), 238–248. https://doi.org/10.1016/j.cej.2009.11.026.

Warchoł, J., Misaelides, P., Petrus, R. & Zamboulis, D. 2006 Preparation and application of organo-modified zeolitic material in the removal of chromates and iodides. *Journal of Hazardous Materials* **137** (3), 1410–1416. https://doi.org/10. 1016/j.jhazmat.2006.04.028.

Wei, W., Sun, R., Jin, Z., Cui, J. & Wei, Z. 2014 Hydroxyapatite– gelatin nanocomposite as a novel adsorbent for nitrobenzene removal from aqueous solution. *Applied Surface Science* **292**, 1020–1029. https://doi.org/10.1016/j.apsusc.2013.12.127.

Zeng, Y., Woo, H., Lee, G. & Park, J. 2010 Removal of chromate from water using surfactant modified Pohang clinoptilolite and Haruna chabazite. *Desalination* **257** (1–3), 102–109. https://doi.org/10.1016/j.desal.2010.02.039.